RESEARCH ARTICLE



Historical trends in the trade wind inversion in the tropical North Atlantic Ocean and Caribbean

Craig A. Ramseyer¹ | Paul W. Miller² |

¹Department of Geography, Virginia Polytechnic Institute and State University, Blacksburg, Virginia

²Department of Oceanography and Coastal Sciences, Louisiana State University, Baton Rouge, Louisiana

Correspondence

Craig A. Ramseyer, Department of Geography, Virginia Polytechnic Institute and State University, 238 Wallace Hall, Blacksburg, VA 24061. Email: ramseyer@vt.edu

Funding information

National Oceanic and Atmospheric Administration Climate Program Office, Grant/Award Number: NA20OAR4310417

Abstract

The trade wind inversion (TWI) serves as an important stabilizing mechanism in the tropical North Atlantic (TNA) region, including the Caribbean basin. Previous studies have diagnosed the TWI using in situ observations and radiosondes, typically over tropical islands. However, studies relying on these point measurements are unable to discern the climatology and evolution of the TWI over the rest of the TNA. This study addresses this gap in the literature through the use of high-resolution ERA5 reanalysis model level data. Due to the advances in the ERA line of reanalysis products, ERA5 now provides vertical level resolution as fine as ~4 mb in the lower troposphere, enabling the identification of shallow inversions, such as the TWI, consistently on a climatological time scale in remote regions of the world. While still coarser than observed soundings, this reanalysis-based approach provides a first attempt in understanding TNA TWI variability and its strength and frequency trends from 1979 to 2019. The TWI climatology constructed here finds consilience with previous modelling and observational studies in terms of the spatial variability of the TWI base and strength across this domain. Stronger and more frequent TWIs are noted across the central TNA across all seasons. Results from a Mann-Kendall analysis reveals increasing trends in TWI frequency and strength that vary spatially across the domain based on season. The most widespread and strongest increasing TWI frequency and strength signal is over the central TNA from December to July. Due to the regionalization of trends noted, potential regional forcing mechanisms responsible for these changes are discussed.

KEYWORDS

decadal variability, ERA5 reanalysis, trade wind inversion, tropical climatology

INTRODUCTION 1

The temperature inversion in the trade wind regime of the tropics and subtropics is a critical atmospheric forcing mechanism. This relatively shallow trade wind inversion (TWI) presents a cap on vertical cloud development as air parcels become negatively buoyant in the layer

(Leopold, 1949; Riehl et al., 1951; Malkus, 1956; Gutnick, 1958; Mendonca and Iwaoka, 1969). In the TWI, the temperature profile is characterized by a positive lapse rate while moisture generally decreases through the layer. The basic model of the TWI is that it lies at the interface between synoptic-scale subsidence from the mid-troposphere and surface-based convective

processes and is particularly strong on the eastern portions of the subtropical oceans (Malkus, 1956; Albrecht, 1984; Carrillo *et al.*, 2016).

The TWI is known to vary diurnally (Riehl et al., 1951; Neiburger et al., 1961), seasonally (Gutnick, 1958; Jordan, 1958; Rouault et al., 2000; Cao et al., 2007; Carrillo et al., 2016), and annually (Cao et al., 2007). The diurnal variability tends to be smaller compared to other temporal modes of variability, as evidenced by studies showing an 85-m difference between morning and afternoon TWI bases (Blake, 1928; Neiburger et al., 1961). Gutnick (1958) was one of the first to show tropical TWIs to be stronger and lower in the winter while weaker and higher in the summer. Cao et al. (2007) detected longer term TWI variability over Hawaii, and showed significant increasing TWI frequency trends during certain seasons, some of which was attributed to internal climate oscillations (e.g., ENSO).

While early studies often discussed the TWI as the sole inversion in the tropical and subtropical domain, more recent studies have shown the tropical troposphere to have a more complex vertical thermodynamic profile. A multiinversion structure has been observed in the temperature profiles of trade-wind soundings (Johnson et al., 1996; Rouault et al., 2000; Carrillo et al., 2016). Studies over the Eastern Atlantic have highlighted the presence of multiple inversions, the two most pronounced at 925 and 800 hPa (Rouault et al., 2000; Carrillo et al., 2016). Those studies indicate that the inversion centered at 925 hPa is denoted by an increase in static stability at the top of the mixing layer, thus not the inversion commonly discussed in the literature as the TWI. Whereas, the increase in stability at 800 hPa is the TWI (Johnson et al., 1996; Carrillo et al., 2016). Previous work included the surface-based (~925 hPa) inversion and showed an upward slope in the TWI base from east-towest across the Atlantic, from a base around 300 m near the coast of Africa above the Canary Current to about 1,500 m in the central portions of the tropical north Atlantic (TNA) (Riehl et al., 1951; Neiburger et al., 1961; Albrecht, 1984). The more recent studies (e.g., Carrillo et al., 2016) would argue that the slope may not be as steep from east-to-west after the removal of the surfacebased inversion.

The TWI has been shown to be a key forcing mechanism for precipitation and convective processes. Studies have found that the TWI prompted horizontal mass divergence (Riehl *et al.*, 1951), negatively buoyant air parcels, and pronounced drying (Gutnick, 1958; von Engeln *et al.*, 2005; Cao *et al.*, 2007). In the Caribbean, observational studies have shown a drying through the TWI layer of 15–30% (Gutnick, 1958), whereas the reduction in moisture has been observed to be as high as 45–50% in Hawaii

(Cao et al., 2007). A kinematic characteristic has also been detected in the TWI layer, showing increased wind shear through the layer (Riehl et al., 1951). More specific to the TNA and Caribbean, the Saharan air layer (SAL) acts as a seasonal TWI modifier as it can influence and modulate the TWI, particularly during the spring and early summer (Prospero and Carlson, 1972, 1981; Dunion and Velden, 2004; Evan et al., 2006; Wong et al., 2009; Chen et al., 2010; Mote et al., 2017; Miller et al., 2021). The direct and indirect aerosol effects associated with the SAL, arising from its high mineral dust concentration, can lead to drought and precipitation reductions across the TNA, even as far as the Caribbean (Mote et al., 2017; Ramseyer et al., 2019). Recent Caribbean hydroclimate studies have shown that precipitation and drought strongly respond to moisture changes in the mid-troposphere (~850-700 hPa) and wind shear through the low- and mid-troposphere (Ramseyer and Mote, 2016, 2018).

However, even the seminal papers of the TNA and Caribbean TWI have identified the feature at disparate locations due to a lack of adequate sounding launch sites across the vast expanse of open ocean (Gutnick, 1958; Jordan, 1958). Unfortunately, even within the Greater and Lesser Antilles island chains, reliable, long-term sounding data are insufficient or nonexistent. Most recent studies in the TNA, including the Caribbean basin, have similarly analysed the TWI at specific geographic locations (e.g., Carrillo et al., 2016), and consequently struggle to represent the two-dimensional evolution of this feature. These studies and others have been critical in understanding the TWI across the TNA and Caribbean, but our understanding of the spatial and temporal heterogeneity in the TWI across the basin has been historically limited by the lack of upper-air data. As such, Schubert et al. (1995) acknowledged that improved understanding of the TWI would be driven by the ability to study its long-term variability. However, the spatial and temporal sparsity of reliable, high-resolution upper-air data has yet to be resolved.

Although climate scientists regularly employ spatially and temporally homogeneous reanalysis products in datalimited regions, legacy reanalysis products have lacked the vertical resolution to capture shallow, TWI-like features. Fortunately, recent advances in data assimilation and computational technology have allowed reanalysis products to improve their vertical resolution. For instance, the resolution in the European Centre for Medium-Range Forecasts (ECMWF) most recent atmospheric reanalysis datasets increased from 60 model levels in ERA-Interim (Dee *et al.*, 2011) to 137 model levels in ERA5 (Hersbach *et al.*, 2020). While not a substitute for sounding data, ERA5 nonetheless assimilates available radiosonde profiles across the basin, with nearby grid points also benefiting

from the in situ data regularly gathered at traditional sounding sites. The purpose of this article is to assess the spatial and temporal morphology and evolution of the TWI across the entire TNA and Caribbean by leveraging the state-of-the-art ERA5 reanalysis.

2 | DATA AND METHODS

Previous work has shown that legacy versions of ECMWF reanalysis validates boundary layer inversion properties in the tropics compared to radio occultation satellite data and radiosondes (von Engeln *et al.*, 2005). The temperature and moisture profiles used to detect atmospheric inversions were acquired from the ERA5 reanalysis dataset (Hersbach *et al.*, 2020), which uses 4D-Var data assimilation in CY41R2 of ECMWF's Integrate Forecast System. ERA5 represents the highest resolution global reanalysis product currently available with 137 hybrid sigma/pressure (model) levels in the vertical from the surface to 0.01 hPa. The vertical levels are highest resolution in the low-troposphere (~4 mb) and coarsen with increasing height.

ERA5 produces atmospheric fields at hourly increments, although, for this study, only the 1,200 UTC and

0000 UTC data from 1980 to 2019 are utilized as finer temporal resolution would yield insignificant changes to atmospheric conditions driving the TWI. ERA5 data were compared to the San Juan, Puerto Rico (TJSJ) sounding from 1980 to 2017 (27,664 soundings analysed) and accurately recreated the temperature profile from San Juan, PR. The TJSJ sounding data were interpolated to the ERA5 model levels. Analysing the layer 950-600 hPa, the nearest ERA5 grid point demonstrated small differences, which may be partially attributable to the displacement between the TJSJ sounding site and the nearest ERA5 grid point (Supplementary Table 1). The differences were less than 1 K at all levels were smallest between 900 and 750 hPa, where most TWIs form, with a mean difference in this layer of 0.24 K. The differences are larger, but still less than 1 K in the boundary layer (likely due to the SJU sounding responding to land surface heating), and above 700 hPa where the ERA5 model levels being to coarsen in resolution.

For this study, the $1^{\circ} \times 1^{\circ}$ ERA5 products were employed over a spatial domain spanning the TNA and most of the Caribbean Sea (Figure 1). Although ERA5 data are also available at finer 0.25° resolution, the basin-scale TWI morphology and synoptic forcings investigated by this study is adequately resolved with the coarser

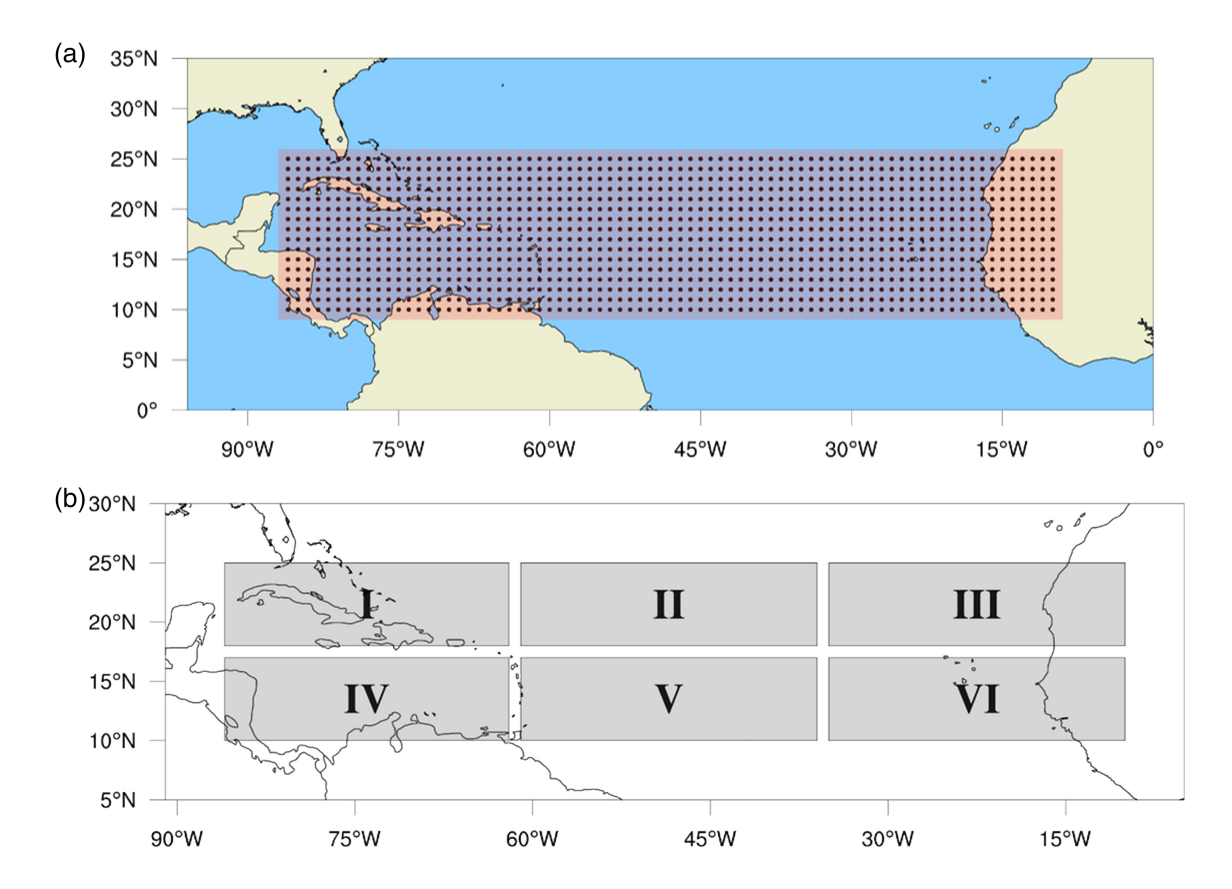


FIGURE 1 (a) Thousand two hundred and thirty two ERA5 grid cells constituting the tropical North Atlantic study area and (b) six embedded subdomains [Colour figure can be viewed at wileyonlinelibrary.com]

products, which are also more easily manipulated. Temperature and specific humidity were acquired for the 137 model levels since postprocessed pressure level data are only available every ~25 mb and lose the ability to adequately resolve the TWI.

The methodology for identifying the TWI largely follows the procedure developed in Cao et al. (2007), summarized below, along with some minor changes made for the TNA domain. First, the inversion height is restricted to 900-600 hPa. This is a slight deviation from previous studies that generally use 950 hPa as a lower bound. The rationale for increasing the lower bound is driven by Johnson et al. (1996) and Carrillo et al. (2016) whom identify two inversions in the eastern tropical Atlantic Ocean above the Canary Current. The lower of the two being produced by sea-surface temperatures boundary-layer processes and thus physically different than the TWI. However, a second inversion is often located above the 900 hPa level, which is more similar to the forcings of the TWI. Consequently, the pressures at all 137 ERA5 model levels were calculated using the contemporaneous ERA5 sea-level pressure field and the L137 model level definitions from ECMWF. Only model levels residing between 900 and 600 hPa were retained.

Lapse rates were calculated using temperature and specific humidity data for all model levels in the 900-600 hPa layer and used to determine the bottom and top of the TWI. Model levels where lapse rates were positive from model level n to model level n + 1 were flagged as possible TWI lower bounds. The depth of the possible TWI increased as lapse rates continued to be greater than zero. Once a negative (or constant) lapse rate was detected, the lower of these two model levels was flagged at the top of the possible TWI. If only one inversion was calculated for the 900-600 hPa layer, it was determined to be the TWI. However, if more than one inversion was detected in the layer, the TWI was determined by which layer was marked by the greatest decrease in specific humidity through the inversion layer. If no inversions were detected, a "no inversion" flag was entered for the gridpoint and timestep. For each TWI, the depth was recorded in meters while the strength of the inversion was estimated by using the total change in temperature (°C) through the layer. On rare occasions, increasing lapse rates were noted at the top of the 900-600 hPa layer, which allowed for flagging it as a TWI, but no other calculations could be performed (depth, strength) as the top of the TWI was located outside the vertical bounds established in this study. A similar process was employed in instances where the lapse rates were positive at the 900 hPa level. These profiles were flagged for having a TWI, but not included in any analysis of TWI depth or strength as a lower bound to the TWI could not be determined. For further details on the TWI detection procedure, refer to Cao *et al.* (2007).

To analyse long-term, statistically significant trends in the ERA5-derived TWI variables, nonparametric Mann-Kendall (MK) tests was performed. The purpose of the MK test (Mann, 1945; Kendall, 1975) is to statistically assess if there is a monotonic increasing or decreasing trend in the TWI variables over time. A monotonic upward (downward) trend indicates that the variable consistently increases (decreases) over time, but it may not be a linear trend. Results are summarized seasonally via three 4-month periods: December-March (DJFM), April-July (AMJJ), and August-November (ASON), which correspond closely to observed precipitation seasonality in the eastern Caribbean (Miller et al. 2019; Miller and Ramseyer, 2020), a region often influenced by the TWI (Jury and Winter, 2010). Although different seasonal definitions may be suggested, the size of the analysis domain captures a large variability in hydroclimatic regimes. Thus, whichever number or length of subannual periods that is appropriate for one region of the domain, may be less appropriate elsewhere; however, this should not preclude a subannual analysis, and so the aforementioned seasons were adopted.

3 | RESULTS AND DISCUSSION

Using the TNA domain and the six sub-TNA regions defined in Figure 1, mean TWI diagnostic characteristics are computed, including TWI base altitude, frequency, and strength. Results for these parameters are presented temporally in terms of both intra-annual variability and long-term trend analysis, as well as spatially over the whole TNA domain. Section 3.3 will compare these ERA5-derived TWI metrics with past studies in the region.

3.1 | TWI climatology

3.1.1 | TWI base

Across all seasons, the ERA5-derived TWI bases indicate a general increase in height from east to west across the domain (Figure 2). The meridional median of the TWI bases indicates an upward slope of the TWI from about ~870 hPa at 30°W (i.e., near the West African coast) to ~780 hPa at 70°W (i.e., in the eastern and central Caribbean), aligning with previous studies that noted the TWI base increases in altitude from east to west across the TNA (Riehl *et al.*, 1951; Neiburger *et al.*, 1961; Albrecht, 1984). Terrestrial grid points (e.g., over land

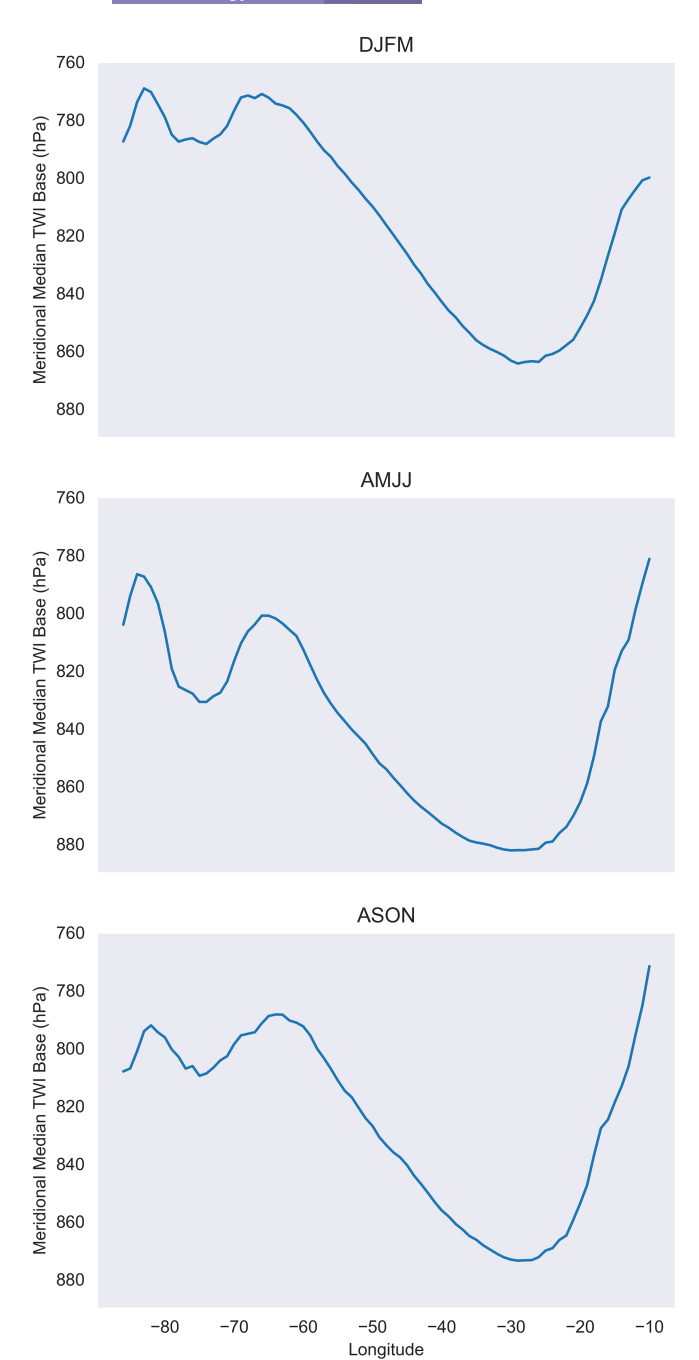


FIGURE 2 Meridional mean TWI base disaggregated by subannual period [Colour figure can be viewed at wileyonlinelibrary.com]

surface) over West Africa are included in the calculation and drive higher TWI bases between 30 and 10°W, as noted in Figure 2. This is likely due to those few grid points also not having a true TWI. These grid points still provide valuable insight on the transition and gradient of the TWI from the West African continent to the adjacent marine environment. Although the east-to-west pattern of increasing TWI base persists across all seasons, the TWI bases are lowest during AMJJ with bases reaching

as low as ~880 hPa in the eastern TNA and ~830 hPa in the Caribbean basin. In contrast, TWI bases are highest TNA-wide during the December–March period, noted for typically dry conditions in the eastern Caribbean (Riehl *et al.*, 1951; Neiburger *et al.*, 1961; Albrecht, 1984; Carrillo *et al.*, 2016).

A persistent undulating pattern to the TWI bases is observed over the western TNA (i.e., the Caribbean basin) during all seasons. After reaching its highest base altitude near 65°W, the TWI base then descends until roughly 75°W before once again rising to a second peak altitude near 80°W. The undulation is strongest during the AMJJ and most dampened during ASON. While the exact values shown here should be used with caution because of the averaging occurring over ~15° latitude, the general slope of the TWI base from east-to-west across the domain provides increased confidence that the ERA5 is resolving TWI bases similarly to observational studies. Possible mechanisms for the reestablishment of the TWI over the western Caribbean and its seasonal variation will be discussed in Section 3.3.

3.1.2 | TWI strength and frequency

described in Section 2, TWI strength and frequency are presented based on the eastern Caribbean seasonal precipitation cycle to assess the intraseasonal variability. In the eastern Caribbean region, the December-March period is drier than the two wet seasons (April-July and August-November), and is driven primarily by increased subsidence and migration of the Inter-Tropical Convergence Zone (ITCZ) out of the domain (Žagar et al., 2011), possibly prompting more frequent and strong TWIs across portions of the domain (Figures 3 and 4). As suggested, the central TNA exhibits signs of frequent and intense TWIs during the DJFM period, centered around 40°W and 16°N (Figure 3) with a tongue of greater TWI frequency, though weaker strength (Figure 4), extending into the Caribbean. During the April-July period, the stronger and frequent TWI signature over the central portion of the domain intensifies (Figures 3 and 4) with TWI strengths estimated over 2.5°C. However, while the mid-TNA TWI strengthens and recurs, the TWI weakens and frequency decreases over the entire Caribbean. A dramatic change in TWI frequency and strength is observed during August-November, with large decreases in both frequency and strength across the entire domain (Figures 3 and 4). The largest magnitude decrease is observed over the central portions of the domain, between 30 and 45°W, where subdegree temperature inversions dominate. TWIs are also less frequent during ASON in this area, and when

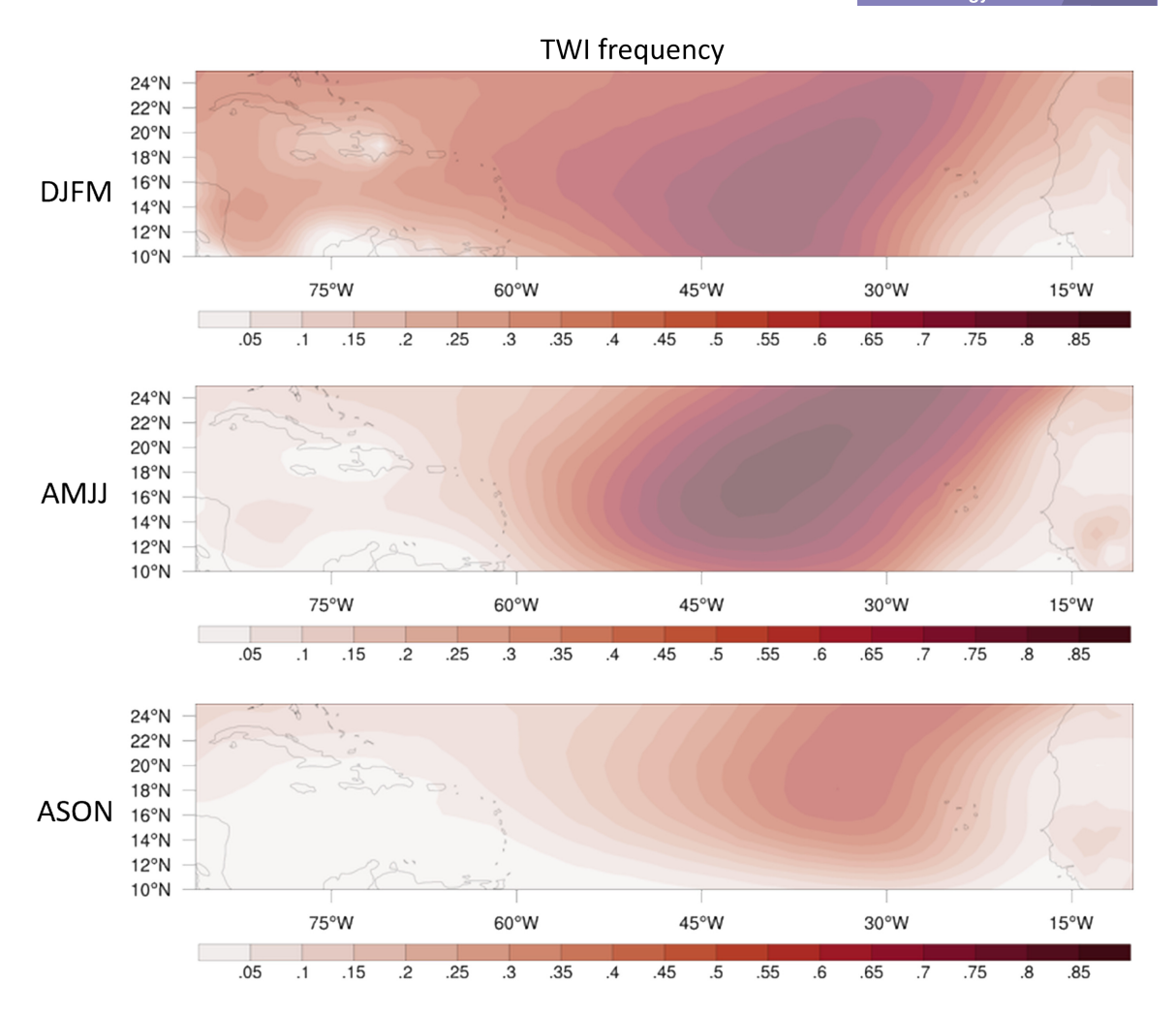


FIGURE 3 Fraction of days with TWI identified disaggregated by subannual period [Colour figure can be viewed at wileyonlinelibrary.com]

TWIs were observed, the strength was decreased by ~1.5°C compared to AMJJ.

3.2 | TWI strength and frequency trends

Because the TWI is such an important hydroclimatic forcing mechanism in the TNA, any trends in TWI strength and/or frequency are particularly relevant for the water-vulnerable landscape in the Caribbean basin. MK tests were conducted to determine temporal trends in TWI morphology over the study area. The analysis will focus only on statistically significant trends while the Kendall τ metric describes the strength of the positive or negative trends. During December–March, only statistically significant increasing TWI frequency and strength trends are identified, and they roughly coincide with the areas of climatologically most frequent and strongest TWIs in the central TNA around 35°W (Figures 5 and 6). Whereas nearly all the grid cells that experienced more

frequency TWIs also witnessed increases in TWI strength, a number of central TNA locations witnessed stronger TWIs, though no increase in frequency (Figures 5 and 6).

The April–July period represents the season with the most grid points showing statistically significant increases in frequency and strength (Figures 5 and 6). TWI frequency is increasing across a large swath of the central Atlantic, just upwind from the eastern Caribbean and Puerto Rico (Figure 5) and west of the area showing increases in TWI frequency during the preceding 4-month window. Another pocket of increasing TWI frequency during the AMJJ is situated over continental sub-Saharan Africa with a few grid points over Saharan Africa demonstrating decreasing TWI frequencies, although, with these grid points being situated over nonmarine surfaces, the inversions being detected here would not be traditionally referred to as the TWI. Meanwhile, the inversion strengthened between 1980 and 2019 during the AMJJ across much of the central TNA,

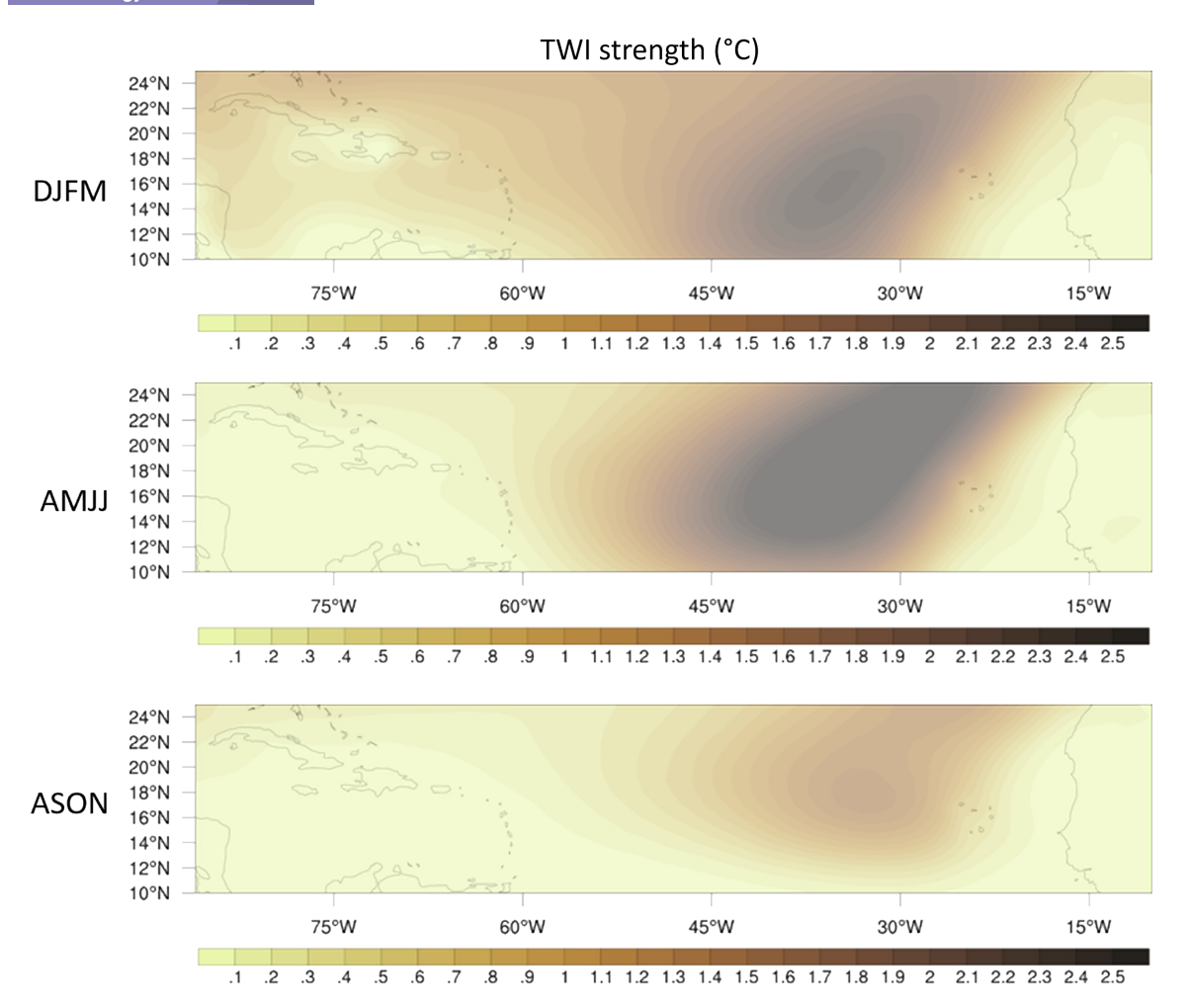


FIGURE 4 Mean TWI strength (°C) on TWI days disaggregated by subannual period [Colour figure can be viewed at wileyonlinelibrary.com]

generally collocated with the inversion frequencies increases, but as with December–March, the area of increasing inversion strength exceeds the areas of increasing inversion frequency. Most of the continental grid points over sub-Saharan Africa also indicate a strengthening inversion during the study period.

The ASON period continues the trends noted during DJFM and AMJJ where all (or nearly all) of the grid points showing statistically significant trends in Figures 5 and 6 are positive (i.e., more frequent, stronger). However, there is a noticeable shift to the southern half of the study domain. Whereas DJFM and AMJJ both noted larger areas of strength increases than frequency increases, the ASON frequency and strength trend maps are much more similar (Figures 5 and 6). While most of the statistically significant trends are located over the central TNA, a tongue of more frequent and stronger TWIs extends into the eastern and central Caribbean. There is a more zonal distribution to the statistically significant grid points compared to the DJFM and AMJJ, which stretches from sub-Saharan Africa to Jamaica.

3.3 | Relationship to possible regional forcing mechanisms

The TWI climatology aligns with the literature as it pertains to the vertical placement of the TWI base and general upward slope across the domain from east-to-west (Figure 2; Riehl et al., 1951; Albrecht, 1984), although those studies did not filter the boundary layer inversions over the Canary Current. However, even as this study removed surface-based inversions, an upward slope is evident. Additionally, the results presented here show the ERA5 climatology is reproducing the seasonal cycle noted previously, with stronger (weaker) inversions in the winter (summer) months (Gutnick, 1958; Cao et al., 2007). In Zones II and V across the Central Atlantic, it appears that TWI may increase in intensity during the late boreal winter and early spring (Figure 6). Additionally, the ERA5 climatology resolves the downwind decreasing intensity of the TWI modelled by Albrecht (1984).

As described in Section 1, the ERA5 climatology offers new insight into the spatial morphology of the TWI

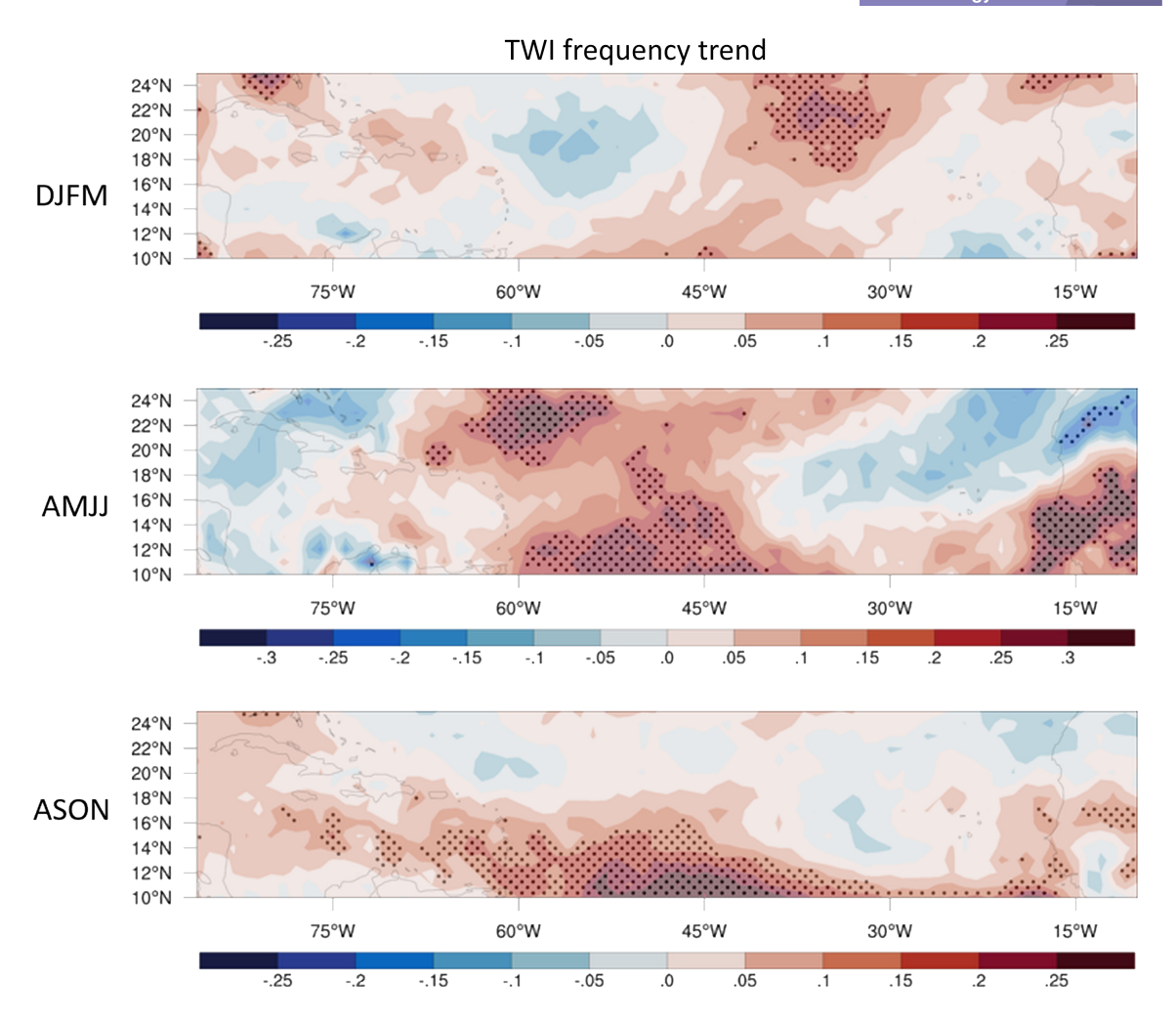


FIGURE 5 TWI frequency trends between 1980 and 2019. Stippled cells indicate locations with statistically significantly increasing or decreasing trends according to the MK test [Colour figure can be viewed at wileyonlinelibrary.com]

across the TNA and the Caribbean. The TWI forms most frequently and strongly across all three seasonal temporal periods in Zones II and V in the central TNA. It is also here that the TWI is becoming more frequent and stronger over the study period, particularly during DJFM and AMJJ (Figures 5 and 6). The statistically significant frequency and strength increases for the ASON period are more confined to Zone V in the extreme southern TNA. Increases in strength and frequency also are detected over continental sub-Saharan Africa during AMJJ in particular. Another more isolated increasing trend is detected during ASON into the Caribbean Sea.

To further understand some of the potential drivers of these TWI trends, additional ERA5 data were retrieved to understand the seasonal evolution of key TWI-related variables: mass subsidence (Figure 7), mass divergence (Figure 8), and humidity (Figure 9). In Zones II and V, mass subsidence is evident in the low- and midtroposphere from December to May (Figure 8b,e) with subsidence remaining quite strong in Zone II through

July (Figure 7b). This is likely driven, in part, by the expansion of the North Atlantic Subtropical High pressure (NASH) into Zone II during the boreal summer, which enhances subsidence in the north-central TNA while subsidence weakens further equatorward. Previous research has found that the NASH has expanded and strengthened over the last several decades in response to anthropogenic warming (Li *et al.*, 2011). When analysing the mass divergence fields, Zone II suggests more persistence in the NASH forcing, encompassing the December–July period with weaker mass divergence during ASON (Figure 8b) when no temporal TWI frequency or strength trends were identified (Figures 5 and 6).

The divergence across Zone V differs during ASON as it appears there is some influence from the northerly migration of the ITCZ (Figure 8e). During this period, mass convergence occurs near the surface in the south-central TNA, which is unusual considering the MK tests revealed a significant increasing trend in both TWI strength and frequency during this time. However, as

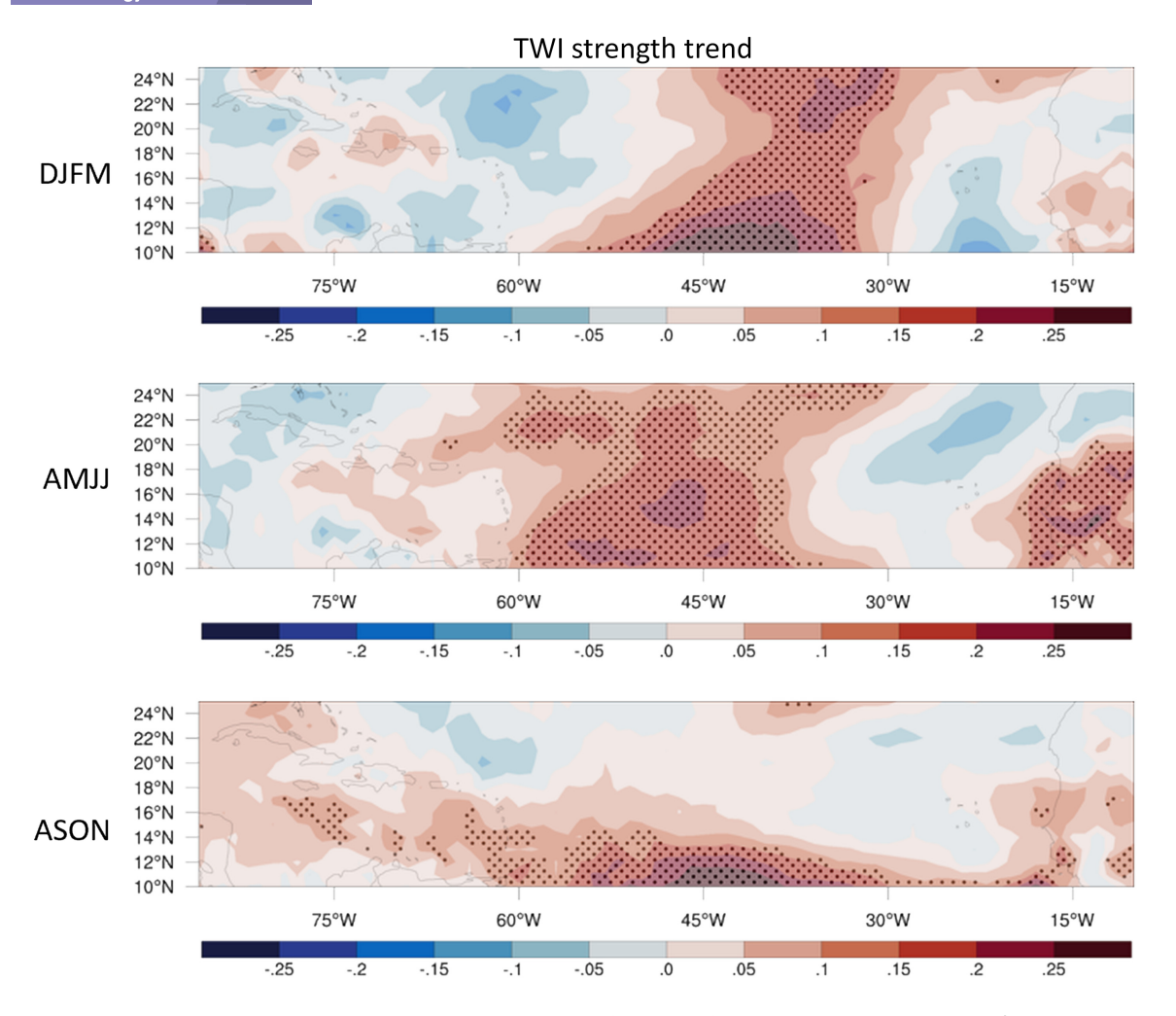


FIGURE 6 TWI strength trends between 1980 and 2019. Stippled cells indicate locations with statistically significantly increasing or decreasing trends according to the MK test [Colour figure can be viewed at wileyonlinelibrary.com]

Figures 3 and 4 indicate, even though the TWI is warming and manifesting more often, it is still a relatively uncommon feature in Zone V during ASON compared to DJFM and AMJJ, which is well explained by the ITCZ signature in Figure 8e. Thus, it is possible that the increasing strength and frequency trends may be related to a shift in the ITCZ during ASON that allows the TWI to form more often. Indeed, Berry and Reeder (2014) identified reductions in ITCZ frequency over the Zone V area between 1979 and 2010.

The vertical relative humidity profiles further contextualize the NASH signal during the DJFM period in particular as mid-troposphere moisture dips significantly in response to the subsidence aloft (Figure 9b,e). Relative humidity in the planetary boundary layer remains relatively high year-round; however, drying is more dramatic from 850 to 500 hPa. While both Zones II and V show increasing moisture through this layer, Zone V has the deeper moist column during ASON which may be additional evidence of some influence from the ITCZ (Figure 9b,e).

The West African Monsoon (WAM) appears to dominate forcings in the eastern portion of the domain, particularly Zone VI. This zone covers portions of the African subcontinent while Zone III is farther north and extends into a climatologically drier regime. In the MK test, Zone VI showed statistically significant changes in TWI strength and frequency, particularly during AMJJ (Figures 5 and 6). Climatologically, during this period, Zone VI often experiences increased upward vertical velocities (i.e., $-\omega$), the most intense in the layer from 925 to 700 hPa (Figure 7f). During ASON, the vertical velocities further intensify and extend throughout the 1,000-500 hPa column, most likely in response to the strong ageostrophic forcing from the WAM (Figure 7f). The surface convergence zone associated with this intense vertical motion drives vertical moisture transport through the low- and mid-troposphere (Figures 9f and 10f). Although the WAM signal is present starting during AMJJ period (Figure 7f), the upward vertical motion is stronger and deeper during ASON, a result

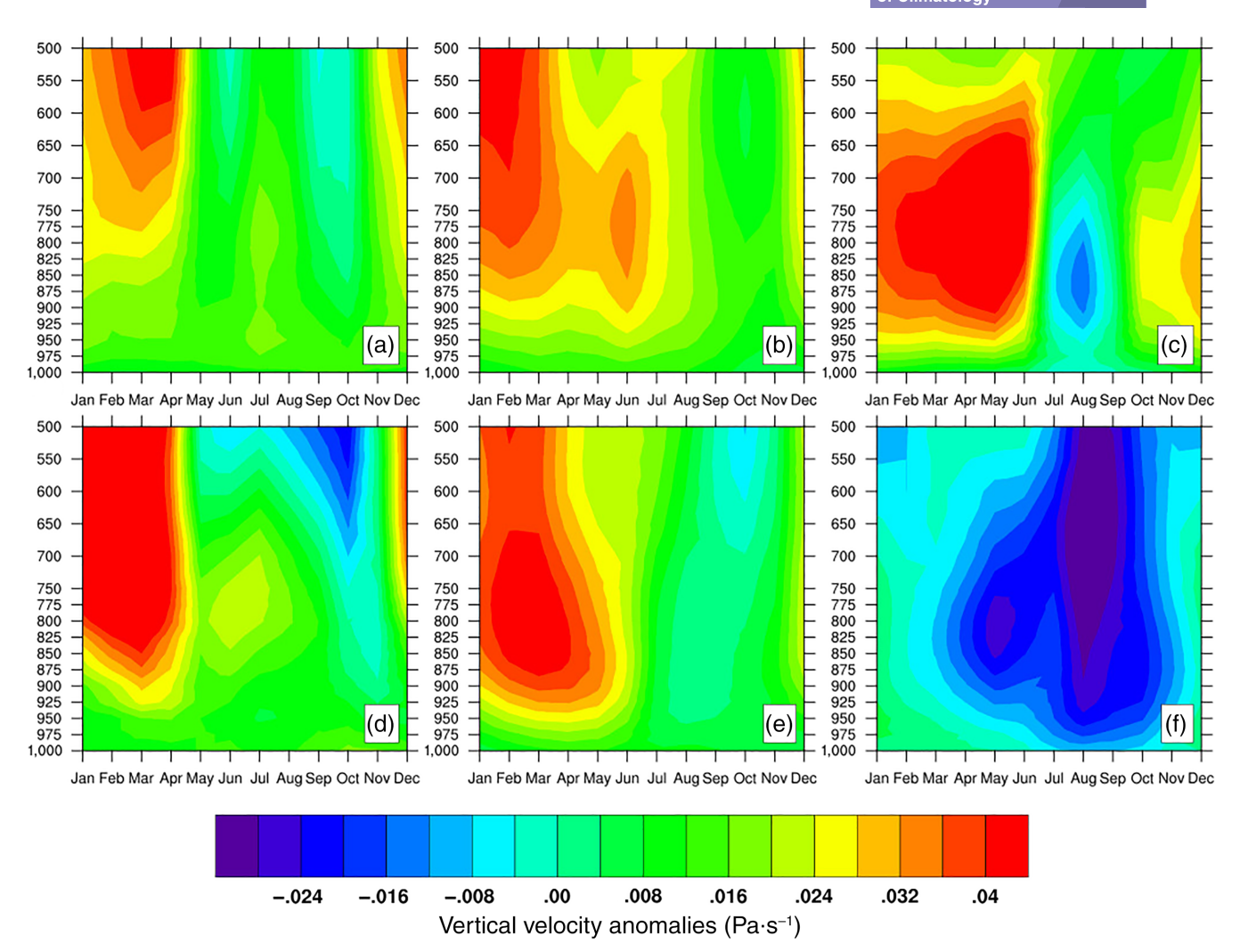


FIGURE 7 Mean vertical velocity (Pa·s⁻¹) between 1980 and 2019 across the annual cycle. Velocity means are disaggregated by the six subregions shown in Figure 1b. Positive (negative) values indicate subsiding (ascending) air [Colour figure can be viewed at wileyonlinelibrary.com]

consistent with previous work (Ramel et al., 2006). The MK tests also detected increasing TWI strength and frequency trends in Zone IV (Figures 5 and 6) although the TWI is not necessarily a strong nor common feature in this zone (Figures 3 and 4). Thus, the changes to TWI morphology in this area may indicate ongoing modifications to the WAM circulation, particularly during the AMJJ period, a possibility detected in global climate simulations (Raj et al., 2019). It should also be noted that this is roughly the same latitude of the strongest SST gradient off the African coast. While this study provides some preliminary evidence that statistically significant increases in TWI frequency and strength are associated with changes to the WAM circulation, further investigations are necessary to address the dynamical adjustments driving these changes.

The western study area (i.e., the Caribbean), covered by Zones I and IV, have the lowest coverage of statistically significant grid points (Figure 5–6), with ASON the only period with increases found within the basin proper. During AMJJ, the eastern Caribbean and Puerto Rico are directly adjacent and downwind to regions of increasing TWI strength and frequency. This 4-month period, a transition window from the DJFM dry season to the much wetter ASON period, experiences weaker subsidence rates (Figure 8a,d) compared to the high-TWI DJFM period (Figure 3). While divergence weakens annually around May, both Zones I and IV show some evidence of a temporary return to renewed lowtropospheric divergence around July. consistent with a distinct Caribbean climatology feature known as the midsummer drought (MSD) or mid-summer dry spell (Curtis and Gamble, 2008; Gamble et al., 2008). From Figure 8a, e, the MSD can be seen as a hydroclimatic response to the mass divergence in July, and alterations to these drivers may also be attributed to the increase in TWI strength and frequency noted during the AMJJ period. The MSD also manifests in the relative humidity fields

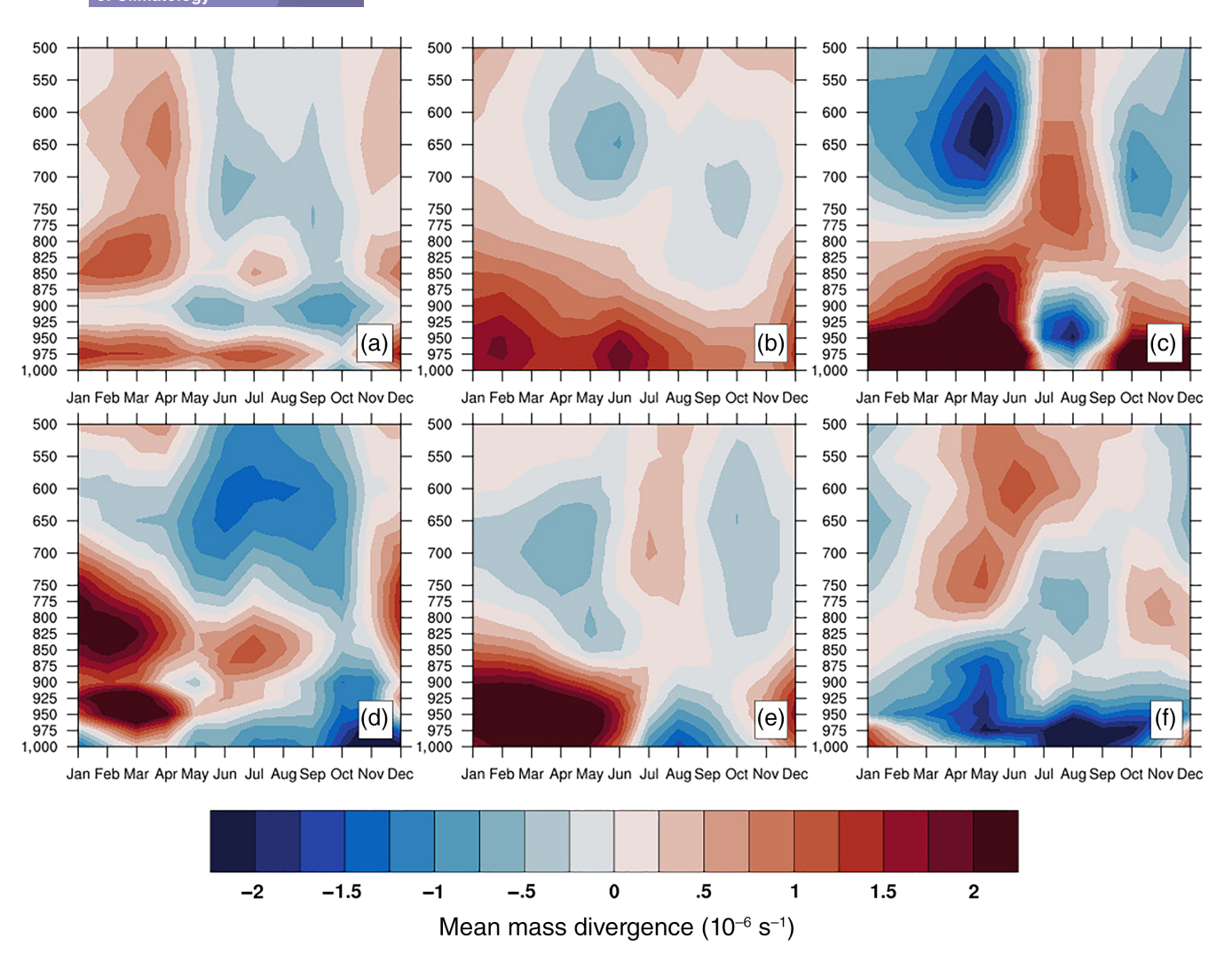


FIGURE 8 Mean mass divergence (10^{-6} s^{-1}) between 1980 and 2019 across the annual cycle. Divergence means are disaggregated by the six subregions shown in Figure 1b. Positive (negative) values indicate divergence (convergence) [Colour figure can be viewed at wileyonlinelibrary.com]

(Figure 10a,d) between 850 and 500 hPa, and as with mass divergence is more clearly apparent in Zone I (Figure 9a).

Zone IV is shown to have grid points with an increasing trend in TWI strength and frequency during ASON. When analysing potential forcing mechanisms, boundary layer mass convergence increases in September (Figure 8d) and is associated with increased upward vertical velocity (Figures 8d) and mid-tropospheric moistening (Figure 9d). However, an additional possibility, the SAL, was mentioned in Section 1. Because the TWI frequency during ASON in Zone IV was so small, even minor increases in TWI occurrence could lead to an increasing trend identified by the MK tests. Although dust transmission from Saharan Africa into the Caribbean is highly seasonal, peaking in June in Barbados and July in Miami, elevated mineral aerosols loadings persist in Zone IV through September (Zuidema *et al.*, 2019).

Recent research has shown that the SAL follows a more northerly route across the TNA between April and October, and additionally, the central latitude of the northerly SAL has moved further north by 0.52° between 2001 and 2015 to near 14.5°N (Meng *et al.*, 2017). Thus, more frequent, though not regular, SAL intrusions into this portion of the domain during the late dust season may be responsible for forming additional inversion layers in the August and September period. Additionally, the SAL may help fortify existing TWIs (Miller *et al.*, 2021). This same logic may also explain the ASON TWI increases in Zone V as well.

The research objectives addressed in this article focus primarily on forcings that impact the annual evolution of the TWI. Based on previous research, the SAL is a seasonal forcing from April to October in this domain and is likely helping to fortify existing TWI structure during those months (Miller *et al.*, 2021). Future work will

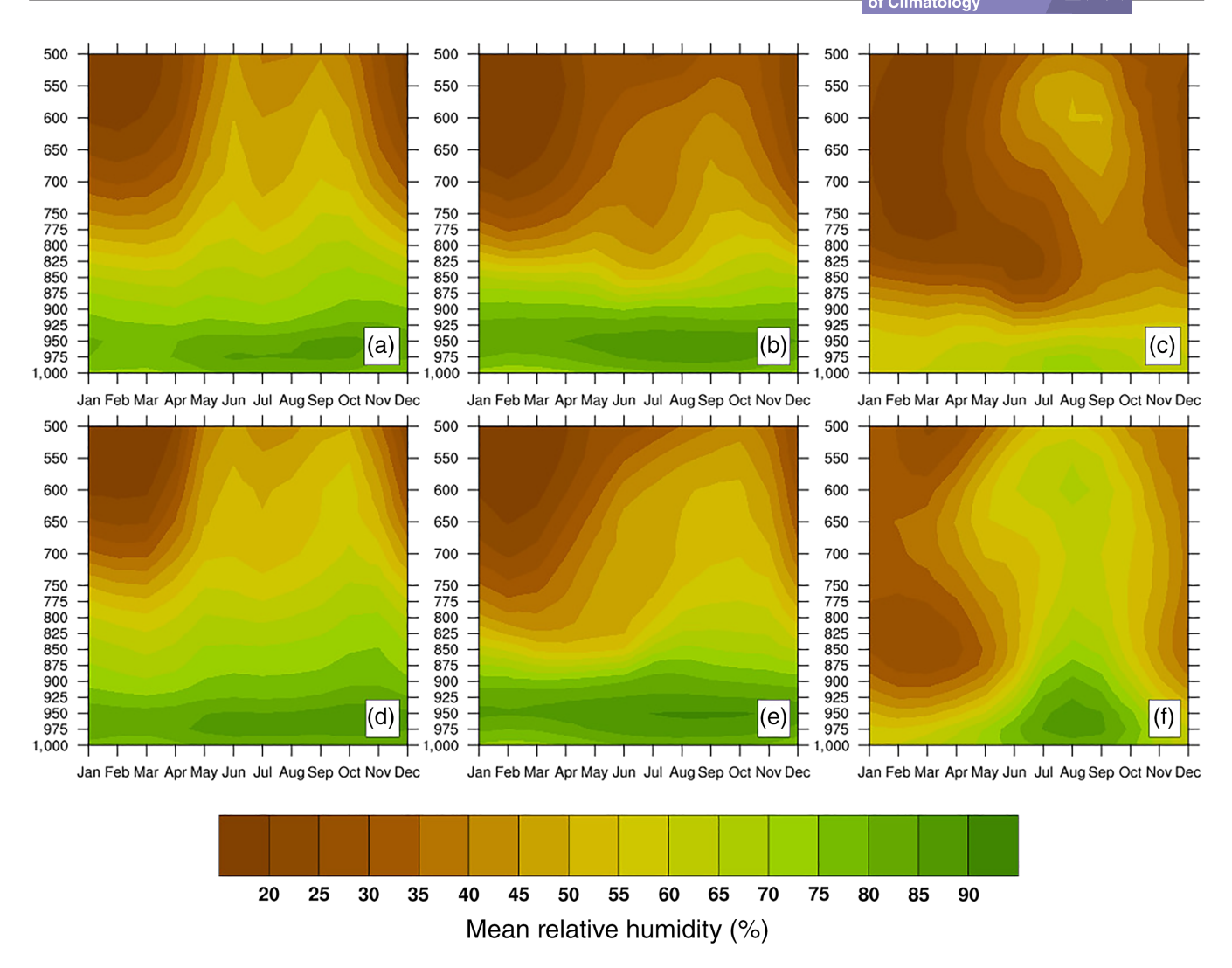


FIGURE 9 Mean relative humidity (%) between 1980 and 2019 across the annual cycle. Humidity means are disaggregated by the six subregions shown in Figure 1b [Colour figure can be viewed at wileyonlinelibrary.com]

design modelling experiments to more adequately address the seasonal forcing SAL imposes on TWI structures in this domain.

4 | CONCLUSIONS

The research presented here builds a spatially contiguous TWI climatology across the greater TNA and Caribbean region. The TWI is also shown to be seasonally varying in frequency and strength. The TWI tends to decrease in strength and frequency moving east-to-west across the study domain. The TWI also decreases in strength and frequency toward the southern TNA as the influence of the ITCZ and WAM prevent TWI formation, particularly during ASON.

The nonparametric MK tests identify statistically significant increasing trends in TWI frequency and strength

within this 40-year dataset across all seasons. These trends are most consistent over the central TNA, likely in response to changes to subsidence driven by midtropospheric forcings from the NASH. However, other dynamical forcings should be further investigated to provide a more thorough understanding of the causes of the intensifying signal. Outside of the central TNA, other subregions have seasonal signals of increasing TWI metrics, particularly in the southern zones where changes to ITCZ and WAM circulations may be altering the TWI. In the Caribbean, increases are noted in ASON. The specific forcings for these regional changes in TWI are the subject of future work, though the SAL, which has also been recently documented to shift to higher latitudes (Meng et al., 2017), is proposed as a possible cause.

TWI morphology has wide ranging impacts across the domain, most notably to precipitation processes. The increasing trends in TWI metrics are likely associated

with changes to the hydroclimate, most notably over the central TNA where the trends are most consistent. In addition to the hydroclimatic impacts, growth of organized convective systems would theoretically be impacted by changes to the TWI regimes, particularly during AMJJ. Additional changes may be possible into the future with anthropogenic climate change and will be evaluated in future studies using global climate model output.

The ERA5-derived TWI trends and associated changes to the underlying forcing mechanisms should be validated by future studies using other reanalysis data or observed soundings in these remote portions of the domain. Of particular interest would be acquiring independent soundings in the central TNA that are not assimilated during the production of the reanalysis data. While a costly endeavour, it would provide a scientifically rigorous validation of the results presented here.

ACKNOWLEDGEMENTS

The authors thank the two anonymous reviewers whose feedback improved this manuscript. This research was supported by a research grant from the NOAA Climate Program Office, Modeling, Analysis, Predictions and Projections Program (NA20OAR4310417).

ORCID

Craig A. Ramseyer https://orcid.org/0000-0003-0290-

Paul W. Miller https://orcid.org/0000-0002-0512-8295

REFERENCES

- Albrecht, B.A. (1984) A model study of downstream variations of the thermodynamic structure of the trade winds. *Tellus A*, 36A(2), 187–202. https://doi.org/10.1111/j.1600-0870.1984.tb00238.x.
- Berry, G. and Reeder, M.J. (2014) Objective identification of the intertropical convergence zone: Climatology and trends from the ERA-interim. *Journal of Climate*, 27(5), 1894–1909. https://doi.org/10.1175/JCLI-D-13-00339.1.
- Blake, D. (1928) Temperature inversions at Sandiego, as deduced from aerographical observations by airplane. *Monthly Weather Review*, 56(6), 221–224. https://doi.org/10.1175/1520-0493(1928) 56<221:TIASDA>2.0.CO;2.
- Cao, G., Giambelluca, T.W., Stevens, D.E. and Schroeder, T.A. (2007) Inversion variability in the Hawaiian trade wind regime. *Journal of Climate*, 20(7), 1145–1160. https://doi.org/10.1175/ JCLI4033.1.
- Carrillo, J., Guerra, J.C., Cuevas, E. and Barrancos, J. (2016) Characterization of the marine boundary layer and the trade-wind inversion over the sub-tropical North Atlantic. *Boundary-Layer Meteorology*, 158(2), 311–330. https://doi.org/10.1007/s10546-015-0081-1.
- Chen, S.-H., Wang, S.-H. and Waylonis, M. (2010) Modification of Saharan air layer and environmental shear over the eastern Atlantic Ocean by dust-radiation effects. *Journal of Geophysical*

- Research: Atmospheres, 115(D21), 1–22. https://doi.org/10.1029/2010JD014158.
- Curtis, S. and Gamble, D.W. (2008) Regional variations of the Caribbean mid-summer drought. *Theoretical and Applied Climatology*, 94(1), 25–34. https://doi.org/10.1007/s00704-007-0342-0.
- Dee, D.P., Uppala, S.M., Simmons, A.J., Berrisford, P., Poli, P., Kobayashi, S., Andrae, U., Balmaseda, M.A., Balsamo, G., Bauer, P., Bechtold, P., Beljaars, A.C.M., van de Berg, L., Bidlot, J., Bormann, N., Delsol, C., Dragani, R., Fuentes, M., Geer, A.J., Haimberger, L., Healy, S.B., Hersbach, H., Hólm, E. V., Isaksen, L., Kållberg, P., Köhler, M., Matricardi, M., McNally, A.P., Monge-Sanz, B.M., Morcrette, J.-J., Park, B.-K., Peubey, C., de Rosnay, P., Tavolato, C., Thépaut, J.-N. and Vitart, F. (2011) The ERA-interim reanalysis: Configuration and performance of the data assimilation system. *Quarterly Journal of the Royal Meteorological Society*, 137(656), 553–597. https://doi.org/10.1002/qj.828.
- Dunion, J.P. and Velden, C.S. (2004) The impact of the Saharan air layer on Atlantic tropical cyclone activity. *Bulletin of the American Meteorological Society*, 85(3), 353–366. https://doi.org/10. 1175/BAMS-85-3-353.
- Evan, A.T., Dunion, J., Foley, J.A., Heidinger, A.K. and Velden, C. S. (2006) New evidence for a relationship between Atlantic tropical cyclone activity and African dust outbreaks. *Geophysical Research Letters*, 33(19), 1–5. https://doi.org/10.1029/2006GL026408.
- Gamble, D.W., Parnell, D.B. and Curtis, S. (2008) Spatial variability of the Caribbean mid-summer drought and relation to North Atlantic high circulation. *International Journal of Climatology*, 28(3), 343–350. https://doi.org/10.1002/joc. 1600
- Gutnick, M. (1958) Climatology of the trade-wind inversion in the Caribbean. *Bulletin of the American Meteorological Society*, 39 (8), 410–420. https://doi.org/10.1175/1520-0477-39.8.410.
- Hersbach, H., Bell, B., Berrisford, P., Hirahara, S., Horányi, A., Muñoz-Sabater, J., Nicolas, J., Peubey, C., Radu, R., Schepers, D., Simmons, A., Soci, C., Abdalla, S., Abellan, X., Balsamo, G., Bechtold, P., Biavati, G., Bidlot, J., Bonavita, M., Chiara, G.D., Dahlgren, P., Dee, D., Diamantakis, M., Dragani, R., Flemming, J., Forbes, R., Fuentes, M., Geer, A., Haimberger, L., Healy, S., Hogan, R.J., Hólm, E., Janisková, M., Keeley, S., Laloyaux, P., Lopez, P., Lupu, C., Radnoti, G., de Rosnay, P., Rozum, I., Vamborg, F., Villaume, S. and Thépaut, J.-N. (2020) The ERA5 global reanalysis. *Quarterly Journal of the Royal Meteorological Society*, 146(730), 1999–2049. https://doi.org/10.1002/qi.3803.
- Johnson, R.H., Ciesielski, P.E. and Hart, K.A. (1996) Tropical inversions near the 0°C level. *Journal of the Atmospheric Sciences*, 53 (13), 1838–1855. https://doi.org/10.1175/1520-0469(1996) 053<1838:TINTL>2.0.CO;2.
- Jordan, C.L. (1958) Mean soundings for the West Indies area. *Journal of Meteorology*, 15(1), 91–97. https://doi.org/10.1175/1520-0469(1958)015<0091:MSFTWI>2.0.CO;2.
- Jury, M.R. and Winter, A. (2010) Warming of an elevated layer over the Caribbean. *Climatic Change*, 99(1), 247–259. https://doi.org/10.1007/s10584-009-9658-3.
- Kendall, M. (1975) Rank Correlation Methods, 4th edition. London: Charles Griffin.

- Leopold, L.B. (1949) The interaction of trade wind and sea breeze, Hawaii. *Journal of Meteorology*, 6(5), 312–320. https://doi.org/10.1175/1520-0469(1949)006<0312:TIOTWA>2.0.CO:2.
- Li, W., Li, L., Fu, R., Deng, Y. and Wang, H. (2011) Changes to the North Atlantic subtropical high and its role in the intensification of summer rainfall variability in the Southeastern United States. *Journal of Climate. American Meteorological Society*, 24 (5), 1499–1506. https://doi.org/10.1175/2010JCLI3829.1.
- Malkus, J.S. (1956) On the maintenance of the trade winds. *Tellus*, 8 (3), 335–350. https://doi.org/10.1111/j.2153-3490.1956.tb01231.x.
- Mann, H.B. (1945) Nonparametric tests against trend. *Econometrica*, 13(3), 245–259. https://doi.org/10.2307/1907187.
- Mendonca, B.G. and Iwaoka, W.T. (1969) The trade wind inversion at the slopes of Mauna Loa, Hawaii. *Journal of Applied Meteorology*, 8(2), 213–219. https://doi.org/10.1175/1520-0450(1969) 008<0213:TTWIAT>2.0.CO;2.
- Meng, L., Gao, H.W., Yu, Y., Yao, X.H., Gao, Y., Zhang, C. and Fan, L. (2017) A new approach developed to study variability in North African dust transport routes over the Atlantic during 2001–2015. *Geophysical Research Letters*, 44(19), 10026–10035. https://doi.org/10.1002/2017GL074478.
- Miller, P., Mote, T. L & Ramseyer, C. A. (2019) An empirical study of the relationship between seasonal precipitation and thermodynamic environment in puerto rico. Weather and Forecasting, 34(2), 277–288.
- Miller, P. & Ramseyer, C. A. (2020) Did the Climate Forecast System anticipate the 2015 Caribbean drought? *Journal of Hydrometeorology*, 21, 1245–1258.
- Miller, P.W., Williams, M. and Mote, T. (2021) Modeled atmospheric optical and thermodynamic responses to an exceptional trans-Atlantic dust outbreak. *Journal of Geophysical Research: Atmospheres*, 126(5), e2020JD032909. https://doi.org/10.1029/2020JD032909.
- Mote, T.L., Ramseyer, C.A. and Miller, P.W. (2017) The Saharan air layer as an early rainfall season suppressant in the Eastern Caribbean: The 2015 Puerto Rico drought. *Journal of Geophysical Research: Atmospheres*, 122(20), 10,966–10,982. https://doi.org/10.1002/2017JD026911.
- Neiburger, M., Johnson, D.S. and Chien, C.W. (1961) Studies of the Structure of the Atmosphere over the Eastern Pacific Ocean. I: The Inversion over the Eastern North Pacific Ocean. Berkeley, CA: University of California Press.
- Prospero, J.M. and Carlson, T.N. (1972) Vertical and areal distribution of Saharan dust over the western equatorial North Atlantic Ocean. *Journal of Geophysical Research* (1896–1977), 77(27), 5255–5265. https://doi.org/10.1029/JC077i027p05255.
- Prospero, J.M. and Carlson, T.N. (1981) Saharan air outbreaks over the tropical North Atlantic. In: Liljequist, G.H. (Ed.) Weather and Weather Maps: A Volume Dedicated to the Memory of Tor Bergeron (15.8.1891–13.6.1977). Basel: Birkhäuser Basel, pp. 677–691.
- Raj, J., Bangalath, H.K. and Stenchikov, G. (2019) West African Monsoon: Current state and future projections in a highresolution AGCM. *Climate Dynamics*, 52(11), 6441–6461. https://doi.org/10.1007/s00382-018-4522-7.
- Ramel, R., Gallée, H. and Messager, C. (2006) On the northward shift of the West African Monsoon. *Climate Dynamics*, 26(4), 429–440. https://doi.org/10.1007/s00382-005-0093-5.
- Ramseyer, C.A., Miller, P.W. and Mote, T.L. (2019) Future precipitation variability during the early rainfall season in the El

- Yunque National Forest. *Science of the Total Environment*, 661, 326–336. https://doi.org/10.1016/j.scitotenv.2019.01.167.
- Ramseyer, C.A. and Mote, T.L. (2016) Atmospheric controls on Puerto Rico precipitation using artificial neural networks. *Climate Dynamics*, 47(7), 2515–2526. https://doi.org/10.1007/s00382-016-2980-3.
- Ramseyer, C.A. and Mote, T.L. (2018) Analysing regional climate forcing on historical precipitation variability in Northeast Puerto Rico. *International Journal of Climatology*, 38(S1), e224–e236. https://doi.org/10.1002/joc.5364.
- Riehl, H., Yeh, T.C., Malkus, J.S. and la Seur, N.E. (1951) The north-east trade of the Pacific Ocean. *Quarterly Journal of the Royal Meteorological Society*, 77(334), 598–626. https://doi.org/10.1002/qj.49707733405.
- Rouault, M., Lee-Thorp, A.M. and Lutjeharms, J.R.E. (2000) The atmospheric boundary layer above the Agulhas current during alongcurrent winds. *Journal of Physical Oceanography*, 30(1), 40–50. https://doi.org/10.1175/1520-0485(2000)030<0040: TABLAT>2.0.CO;2.
- Schubert, W.H., Ciesielski, P.E., Lu, C. and Johnson, R.H. (1995)

 Dynamical adjustment of the trade wind inversion layer.

 Journal of the Atmospheric Sciences, 52(16), 2941–2952.

 https://doi.org/10.1175/1520-0469(1995)052<2941:

 DAOTTW>2.0.CO;2.
- von Engeln, A., Teixeira, J., Wickert, J. and Buehler, S.A. (2005) Using CHAMP radio occultation data to determine the top altitude of the planetary boundary layer. *Geophysical Research Letters*, 32(6), 1–4. https://doi.org/10.1029/2004GL022168.
- Wong, S., Dessler, A.E., Mahowald, N.M., Yang, P. and Feng, Q. (2009) Maintenance of lower tropospheric temperature inversion in the Saharan air layer by dust and dry anomaly. *Journal of Climate*, 22(19), 5149–5162. https://doi.org/10.1175/2009JCLI2847.1.
- Žagar, N., Skok, G. and Tribbia, J. (2011) Climatology of the ITCZ derived from ERA interim reanalyses. *Journal of Geophysical Research: Atmospheres*, 116(D15), 1–6. https://doi.org/10.1029/2011JD015695.
- Zuidema, P., Alvarez, C., Kramer, S.J., Custals, L., Izaguirre, M., Sealy, P., Prospero, J.M. and Blades, E. (2019) Is summer African dust arriving earlier to Barbados? The updated long-term in situ dust mass concentration time series from ragged point, Barbados, and Miami, Florida. Bulletin of the American Meteorological Society, 100(10), 1981–1986. https://doi.org/10.1175/BAMS-D-18-0083.1.

SUPPORTING INFORMATION

Additional supporting information may be found online in the Supporting Information section at the end of this article.

How to cite this article: Ramseyer CA, Miller PW. Historical trends in the trade wind inversion in the tropical North Atlantic Ocean and Caribbean. *Int J Climatol*. 2021;41:5752–5765. https://doi.org/10.1002/joc.7151